

Possibility of superconductivity in graphite intercalated with alkaline earths investigated with density functional theory.

Matteo Calandra and Francesco Mauri

Institut de Minéralogie et de Physique des Milieux condensés,
case 115, 4 place Jussieu, 75252, Paris cedex 05, France
(Dated: April 15, 2024)

Using density functional theory we investigate the occurrence of superconductivity in AC_6 with $A = Mg, Ca, Sr, Ba$. We predict that at zero pressure, Ba and Sr should be superconducting with critical temperatures (T_c) 0.2 K and 3.0 K, respectively. We study the pressure dependence of T_c assuming the same symmetry for the crystal structures at zero and finite pressures. We find that the SrC_6 and BaC_6 critical temperatures should be substantially enhanced by pressure. On the contrary, for CaC_6 we find that in the 0 to 5 GPa region, T_c weakly increases with pressure. The increase is much smaller than what shown in several recent experiments. Thus we suggest that in CaC_6 a continuous phase transformation, such as an increase in staging, occurs at finite pressure. Finally we argue that, although MgC_6 is unstable, the synthesis of intercalated systems of the kind $Mg_xCa_{1-x}C_y$ could lead to higher critical temperatures.

PACS numbers: 63.20.Kr, 63.20.Dj, 78.30.Er, 74.70.Ad

I. INTRODUCTION

It has long been known that Graphite intercalated compounds (GICs) can display a superconducting behavior at low temperature¹. However, until the discovery of ytterbium and calcium intercalated graphite^{2,3} ($T_c(YbC_6) = 6.5$ K and $T_c(CaC_6) = 11.5$ K), the critical temperatures achieved were typically inferior to 5 K elvin. Very recently, it has been shown that even higher critical temperatures (up to 15.1 K) can be achieved in CaC_6 applying hydrostatic pressure (up to 8 GPa)⁴. This is presently the highest T_c reported in a GIC.

From a practical point of view GICs are appealing since carbon is a very versatile element. Beside the fact that the three most known carbon crystalline structures (Fullerene, Graphite and Diamond) display superconducting behavior upon intercalation^{1,5} or doping⁶, carbon is also interesting for the possibility of making nanotubes which can display a superconducting behavior⁷. Moreover the number of reagents which can be intercalated in graphite, by using chemical methods or high pressure synthesis, is very large. Consequently finding GICs with even higher critical temperatures is not a remote possibility. Therefore theoretical calculations can be a precious tool for the investigation of superconductivity in GICs.

The nature of superconductivity in intercalated GICs is still controversial. Due to their layered nature and to the presence of an intercalant band at the Fermi level (E_F), Csanayiet al.⁸ suggested a non-conventional exciton pairing mechanism⁹. On the contrary Mazin¹⁰ proposed an electron-phonon mechanism mainly sustained by Ca vibration. In a previous work¹¹ we suggested that the pairing is mediated by the electron-phonon interaction. In particular the carriers are mostly electrons in the Ca Fermi surfaces coupled with Ca in-plane and C-out of plane vibrations. The calculation of the isotope effect coefficient showed that the contribution of Ca in-plane

vibrations and C out-of-plane vibrations to superconductivity is comparable.

Experimental data seem to confirm that the pairing in CaC_6 and YbC_6 is indeed due to the electron-phonon interaction, but several open questions remain. From the exponential behavior of the penetration depth in CaC_6 Lamura et al.¹² deduced an isotropic gap of magnitude $\Delta(0) = 1.79 \pm 0.08$ meV. A similar isotropic gap ($\Delta(0) = 1.6 \pm 0.2$ meV) has been measured by scanning tunneling spectroscopy¹³. The corresponding values of $2\Delta(0) = T_c$ are in agreement with the BCS theory. Similar conclusions have been obtained from the specific heat jump at superconducting transition¹⁴. Thermal conductivity data in the presence of a magnetic field¹⁵ indicate that in YbC_6 the order parameter has s-wave symmetry too and exclude the occurrence of multiple gaps. Isotope effect measurements¹⁶ show a huge Ca isotope coefficient, $\alpha(Ca) = 0.5$, in disagreement with theoretical calculations¹¹. This is surprising, since the gap and specific heat data are correctly described by DFT calculations, meaning that the calculated electron-phonon coupling is probably correct. Even more interesting is that the total isotope effect would be probably larger than 0.5, although C-isotope effect measurements are necessary to confirm this and to judge the validity of the measurements of $\alpha(Ca)$. In any case, the large Ca-isotope coefficient, the measured superconducting gap and the jump of the specific heat at the transition they all go in favor of a phonon mediated mechanism with, most likely, a single s-wave gap.

In this work we want to push a step forward the prediction that can be made by the electron-phonon theory. This is important since it may allow to identify GICs with higher critical temperatures and it also represents a significative benchmark for DFT simulations. It was noted⁸ that all the superconducting GICs possess an intercalant Fermi surfaces at E_F . This fact is relevant for both pairing mechanism proposed. In the case of a con-

ventional electron-phonon mechanism the electrons in the intercalant Fermi surface are the ones strongly coupled to the phonons¹¹. Thus we study the possible occurrence of superconductivity in graphite intercalated with alkaline earths (AC_6 with $A = \text{Ba, Sr, Mg}$). All these GICs have an intercalant Fermi surface at E_f so they are good candidates for superconductivity. We predict the critical temperatures for BaC_6 and SrC_6 in the framework of the electron-phonon coupling theory.

As mentioned before, the critical temperature of CaC_6 and YbC_6 is enhanced with pressure. Resistivity measurements under pressure show that, at 8 GPa, CaC_6 undergoes a structural phase transition to a new superconducting phase with a lower critical temperature. The new structure seems to be stable at least up to 16 GPa. In other successive works magnetic^{17,18} and resistive¹⁸ measurements were performed in a much smaller range of pressures (0-1.6 GPa) and the behavior observed was confirmed. Pressure also increases the critical temperature of YbC_6 up to approximately 7.0 K at 2.0 GPa. In this case too a structural transition is seen towards a new superconducting phase with lower T_c . In both YbC_6 and CaC_6 the dependence of T_c is linear with similar $T_c = P$ (0.4 for YbC_6 and 0.5 for CaC_6). The fact that T_c can be enhanced with pressure suggests that this can be a general mechanism for superconducting in GICs. It is then important to study superconductivity as a function of pressure in BaC_6 , SrC_6 and finally CaC_6 .

After illustrating in section II and III the technical parameters and the lattice structures used in the simulations, we study the electronic structure (sec. IV), the phonon dispersions (sec. V) and the superconducting properties (sec. VI) of Alkaline-earth intercalated graphite at ambient pressure and at finite pressure. Particular emphasis is given to the case of CaC_6 under pressure (sec. VII).

II. TECHNICAL DETAILS

Density Functional Theory (DFT) calculations are performed using the *espresso* code¹⁹ and the generalized gradient approximation (GGA)²⁰. We use ultrasoft pseudopotentials²¹ with valence configurations $3s^2 3p^6 4s^2$ for Ca, $4s^2 4p^6 4d^1 5s^1 5p^0$ for Sr, $5s^2 5p^6 5d^0 6s^2 6p^0$ for Ba, and $2s^2 2p^2$ for C. For Mg we use Troullier-Martin²² pseudopotentials with configuration $3s^{0.1} 3p^0 3d^0$. The wavefunctions and the charge density are expanded using a 35 Ry and a 600 Ry cutoff. The dynamical matrices and the electron-phonon coupling are calculated using Density Functional Perturbation Theory in the linear response¹⁹. For the electronic integration in the phonon calculation (structure $R\bar{3}m$) we use a $N_k = 6 \times 6 \times 6$ and $N_k = 8 \times 8 \times 8$ uniform k -point meshes and Hermite-Gaussian smearing ranging from 0.1 to 0.05 Ry. In order to obtain very accurate phonon-frequencies for the low energy modes (below 15 meV) it is crucial to use a large cutoff for the charge density (600 Ry at least)

and a very high convergence threshold in the phonon calculations. For the evaluation of the electron-phonon coupling and of the electronic density of states we use $N_k = 25 \times 25 \times 25$ and $N_k = 20 \times 20 \times 20$ meshes respectively. For the average over the phonon momentum q we use a $N_q = 4 \times 4 \times 4$ q points mesh. The phonon dispersion is obtained by Fourier interpolation of the dynamical matrices computed on the N_q mesh.

III. CRYSTAL STRUCTURE

All the considered compounds are stage 1¹ at zero pressure. The atomic structure³ of CaC_6 involves a stacked arrangement of graphene sheets (stacking AAA) with Ca atoms occupying interlayer sites above the centers of the hexagons (stacking $\sqrt{3} \times \sqrt{3}$). The crystallographic structure is $R\bar{3}m$ where the Ca atoms occupy the 1a Wyckoff position (0,0,0) and the C atoms the 6g positions ($x, -x, 1/2$) with $x = 1/6$. SrC_6 and BaC_6 have a slightly different crystal structure²³ involving a stacked arrangement of graphene sheets (stacking AAA) with Sr and Ba atoms occupying interlayer sites above the centers of the hexagons with an $\sqrt{3} \times \sqrt{3}$ stacking. The crystallographic structure is $P6_3/mmc$ where the Sr/Ba atoms occupy the 2c Wyckoff position (1/3, 2/3, 1/4) and (1/3, 2/3, 3/4) and the C atoms the 12i positions (1/3, 0, 0). The experimental in plane lattice parameter a and the interlayer spacing c for the three structures are illustrated in table I.

Material	Stacking	a, c	a, c (LDA)	a, c (GGA)
BaC_6	AA	4.302 5.25	4.280 5.00	4.350 5.20
SrC_6	AA	4.315 4.95	4.285 4.80	4.325 5.00
CaC_6	AAA	4.333 4.524	4.29 4.36	4.333 4.51
MgC_6			4.317 3.75	4.35 3.95

TABLE I: Experimental (first two columns) structural parameters (Angstrom) of BaC_6 , SrC_6 , CaC_6 . With c we indicate the interlayer spacing, namely the distance between two graphene layers, while a is the in plane lattice parameter. In the last two columns we report the parameters of the theoretical (LDA and GGA) $R\bar{3}m$ structure (stacking AAA) having the same a and the same interlayer distance of the experimental structure. This rhombohedral structure is considered in all the calculations. Since MgC_6 has never been synthesized we only report its theoretical minimized structure with symmetry $R\bar{3}m$.

Even if the structural symmetry of SrC_6 and BaC_6 are different from the one of CaC_6 , in this work we consider the same rhombohedral symmetry group (namely $R\bar{3}m$ with stacking AAA) for all the considered GICs. We do not expect this assumption to affect qualitatively the calculated electronic and phonon properties since the two structures differ only for large distance neighbors. Indeed the distances of the first and second nearest neighbors are the same. The differences between the metal lattice sites in the AAA and in the AA structures is equivalent to those existing in the fcc and in the hcp structures.

System	Pressure (GPa)	a	c
BaC ₆	8	4.287	4.925
SrC ₆	8	4.295	4.750
	16.5	4.265	4.524
CaC ₆	3	4.333	4.524
	5	4.317	4.349
	6	4.314	4.330
	7	4.310	4.301
	8	4.307	4.290
	9	4.303	4.270
	10	4.300	4.250

TABLE II: Theoretical (GGA) Structure of Alkali-earth GICs under pressure

In the last three columns of table I we report the theoretically minimized parameters assuming the R3m structure and using the local density approximation (LDA) or the Generalized-Gradient approximation (GGA). The interlayer distance between graphite layers (c) and the in-plane lattice parameter (a) calculated with GGA are in very good agreement with experiments. The equilibrium LDA a and c parameters are slightly compressed respect to the CGA and experimental values.

Since MgC₆ has never been synthesized, we also assume that it crystallizes in the R3m structure. The theoretical equilibrium parameters are reported in table I. We have verified that this structure is unstable since its energy in CGA is lower by 0.016 Ry/(Cell CaC₆) than the ones of Magnesium and Graphite separated.

In Alkali-earth GICs as the atomic number of the intercalant (Z) is reduced the c parameter is also reduced. To disentangle the two effects we consider BaC₆, SrC₆ and CaC₆ under isotropic pressure. Since the structure of these systems at a given pressure is not known, we minimize the R3m structure at a given isotropic pressure. The lattice parameters obtained are illustrated in table II. It should be noticed that for SrC₆ the pressure of 16.5 GPa has been chosen since the c parameter has the same value as in CaC₆ at zero pressure.

When possible, we always used the experimental a and c parameters in the electronic structure calculations. When lacking, we used the GGA minimized parameters.

IV. ELECTRONIC STRUCTURE

The zero-pressure DFT-band-structures of the Ba, Sr, Ca, Mg intercalated compounds are illustrated in fig. 1. All the considered alkali-earth intercalated GICs have at least one intercalant band at the Fermi level. This was proposed to be^{8,11} a necessary condition in order to have superconductivity with a reasonable critical temperature in GICs.

The considered GICs are layered structures, but their band structure are clearly three-dimensional. This was understood in the case of CaC₆¹¹ since the rhombohedral

angle (49.55°) is not too far from the one corresponding to the fcc structure (60°). The rhombohedral angles for BaC₆, SrC₆ and MgC₆ are 43.47°, 45.81°, 55.37°, respectively. Thus the rhombohedral angle is larger as c is reduced. This is even more evident comparing the behavior of the band-structure as a function of pressure in fig. 2 for SrC₆. Note in particular, that at 16.5 GPa (where the c parameter is the same as that of CaC₆ at zero pressure) the band structure is very similar to the one of CaC₆ at zero pressure. The larger bandwidths of the intercalant band as c is reduced reflects the higher three dimensional character of the structure.

The electronic density of states for the four considered compounds are very similar (see fig. 1) and also their values at the Fermi level are very close. No qualitative difference in the superconducting behavior of these systems can be attributed to the number of carriers at the Fermi energy (i.e. to the different value of N(0)).

The atomic-projected density of states is calculated using the Lowdin populations, $\rho_i = \frac{1}{N} \sum_{\mathbf{k}} \sum_{\mathbf{l}} |j_{\mathbf{k}\mathbf{l}}|^2$ (\mathbf{k}, \mathbf{l}). In this expression $j_{\mathbf{k}\mathbf{l}} = \langle \phi_{\mathbf{k}} | S_{\mathbf{l}} | \phi_{\mathbf{l}} \rangle$ are the orthonormalized Lowdin orbitals, $\phi_{\mathbf{l}}$ are the atomic wavefunctions and $S_{\mathbf{l}} = \sum_{\mathbf{a}} |a\rangle \langle a|$. The density of states projected over the intercalant states has very similar value at E_f for the three cases and it is slightly reduced with decreasing Z. No particular differences respect to the case of CaC₆ are observed¹¹. In fig. 1 (right) the size of the dots represents the projection over the intercalant atomic states.

The three Fermi surface sheets of BaC₆, SrC₆ and CaC₆ are shown in fig. 3. The sheets have been identified by the corresponding band index. As c is reduced passing from BaC₆ to CaC₆ the main difference is the change in the third sheet of the Fermi surface which is indeed a warped cylinder in BaC₆ and it becomes spherical in CaC₆. This is best seen analyzing the band structure in the L direction (namely the k_z direction). In BaC₆ and SrC₆ there are no bands crossing E_f along L, while in CaC₆ the Ca-originated band crosses E_f .

V. PHONON DISPERSION

The phonon dispersion of all the considered GICs can be divided in three regions. The high energy region is composed by in-plane Carbon-vibration (C_{xy}), the intermediate energy region by out-of-plane Carbon vibration (C_z), and the low energy region is mostly composed intercalant vibration (I_{xy} for in-plane and I_z for out-of-plane, with I=Ba, Sr, Ca, Mg), as it was shown for CaC₆¹¹. Since the high energy branches ($\hbar\omega > 100$ meV) are weakly affected by the type of intercalant, for the sake of clarity, in some cases we only plot branches in the low energy region of the spectra. These branches are those having the greatest contribution to the electron-phonon coupling.

The zero-pressure phonon dispersion of BaC₆, SrC₆ and CaC₆ are illustrated in figs. 4 and 5. As Z is reduced,

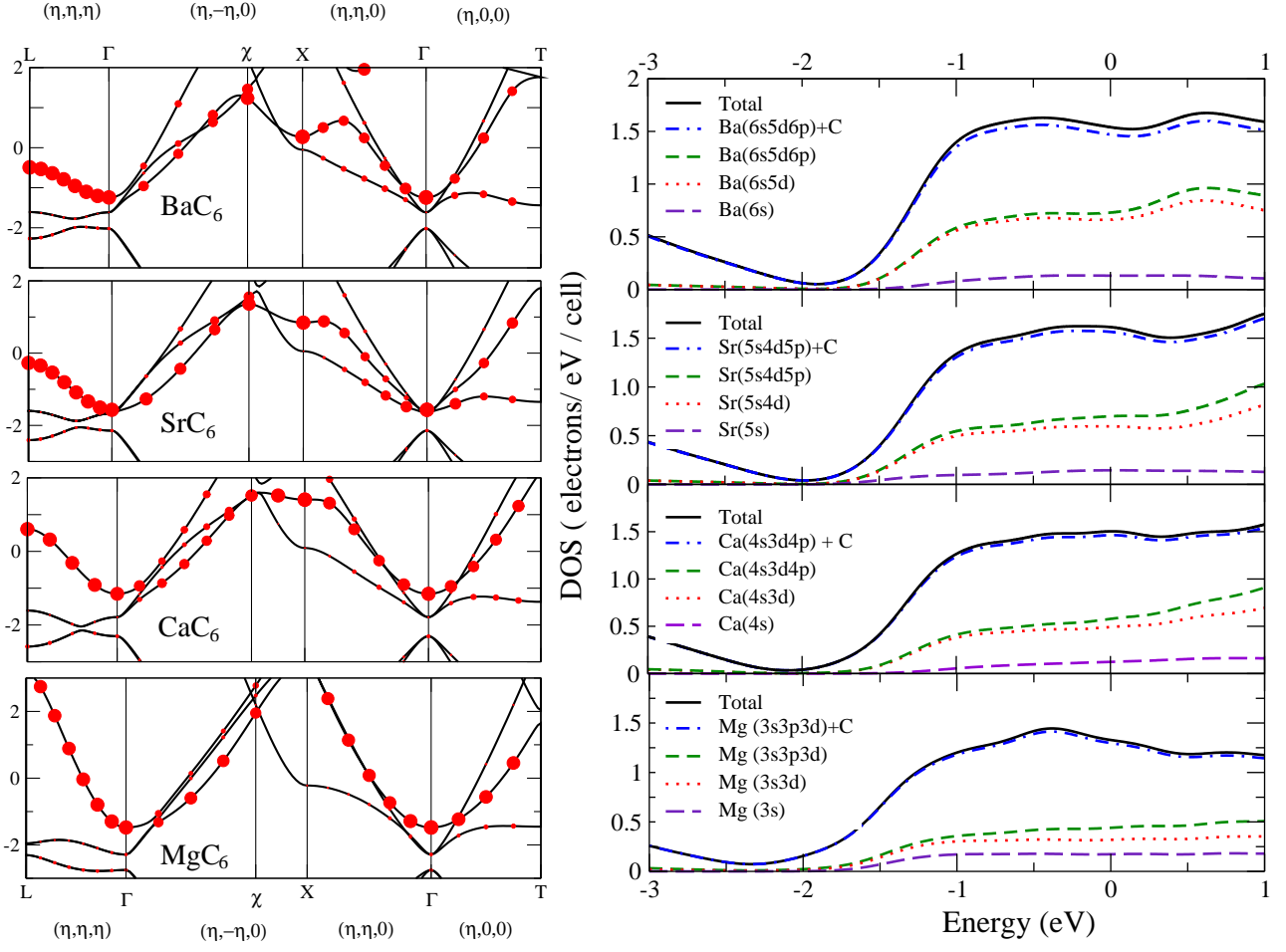


FIG. 1: (Color online) Band structure (left) and density of states projected over atomic orbitals (right) for several Alkali-Earths GICs. The zero energy corresponds to the Fermi energy. The size of the dots represents the percentage of intercalant component. As a reference, in CaC_6 the dot at -0.6eV at the L point represents 95%.

and consequently c is reduced, the lowest energy branch in the X direction (which corresponds to in-plane momenta with $k_z = 0$) is softened. This is evident in CaC_6 where an incipient Kohn anomaly is found at X. While the reduction of c or Z softens the I_{xy} , the intercalant I_z out-of-plane vibrations are hardened.

This effect is also apparent from the analysis of the phonon dispersion of SrC_6 and CaC_6 under pressure. In SrC_6 the lowest branch at 16 GPa in the X direction is almost imaginary, meaning that at this pressure the system is close to a structural instability²⁴. This instability is driven by the reduction in the c -lattice spacing. In MgC_6 , at the theoretical lattice parameters I , we find imaginary phonon frequencies at X, so that the system is probably unstable. As a consequence we did not calculate the full phonon dispersion.

VI. SUPERCONDUCTING PROPERTIES

The superconducting properties of Alkali-Earths GICs can be understood calculating the electron-phonon cou-

pling λ_q for a phonon mode with momentum q :

$$\lambda_q = \frac{4}{N} \sum_{k, m, n} \frac{1}{N_k} \langle \mathbf{r}_{k, n} | \mathbf{r}_{k+q, m} \rangle \langle \mathbf{r}_{k, n} | \mathbf{r}_{k+q, m} \rangle \quad (1)$$

where the sum is over the Brillouin Zone. The matrix element is $g_{k, n, k+q, m} = \langle \mathbf{r}_{k, n} | \mathbf{r}_{k+q, m} \rangle = \langle \mathbf{r}_{k, n} | \mathbf{r}_{k+q, m} \rangle$, where u_q is the amplitude of the displacement of the phonon and V is the Kohn-Sham potential. The average electron-phonon coupling is $\lambda = \sum_q \lambda_q / N_q$ and its value for the different compounds and for different pressures is given in table IV.

The Eliashberg function

$$\alpha^2 F(\omega) = \frac{1}{2N_q} \sum_q \lambda_q \delta(\omega - \omega_q) \quad (2)$$

and the integral $\lambda(\omega) = 2 \int_0^\omega \alpha^2 F(\omega') d\omega'$ are shown in Fig. 7 for BaC_6 and SrC_6 . As for CaC_6 the largest contribution to λ comes from modes below 75 meV.

An estimate of the different contributions of the in-plane and out-of-plane vibrations of the different atoms

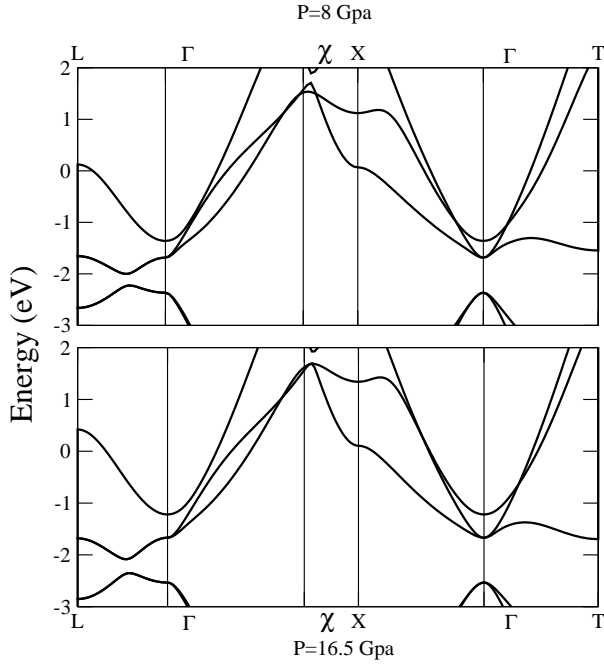


FIG. 2: Band structure of SrC_6 at different pressures. The zero of the energy corresponds to the Fermi energy

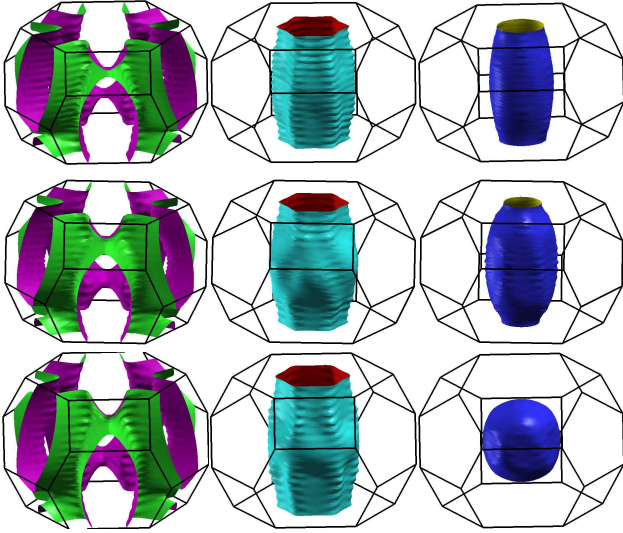


FIG. 3: (Color online) Fermi surface sheets of BaC_6 , SrC_6 and CaC_6 at zero pressure. The sheets are plotted in order of increasing band index.

to can be obtained from the relation

$$= \frac{1}{N_q} \sum_{q, i, j} \mathbf{G}_{q, i, j} \mathbf{C}_{q, i, j}^{-1} \quad (3)$$

where i, j indexes indicate the displacement in the Cartesian direction of the i^{th} atom, $\mathbf{G}_{q, i, j} = \frac{1}{N} \sum_{\mathbf{k}} \mathbf{g}_i(\mathbf{k}) \mathbf{g}_j(\mathbf{k} + \mathbf{q}) e^{i\mathbf{q} \cdot (\mathbf{r}_i - \mathbf{r}_j)}$, and $\mathbf{g}_i = \frac{1}{\sqrt{N}} \sum_{\mathbf{k}} \mathbf{f}_i(\mathbf{k}) e^{i\mathbf{k} \cdot \mathbf{r}_i}$. The \mathbf{C}_q matrix is the Fourier transform of the force constant matrix (the

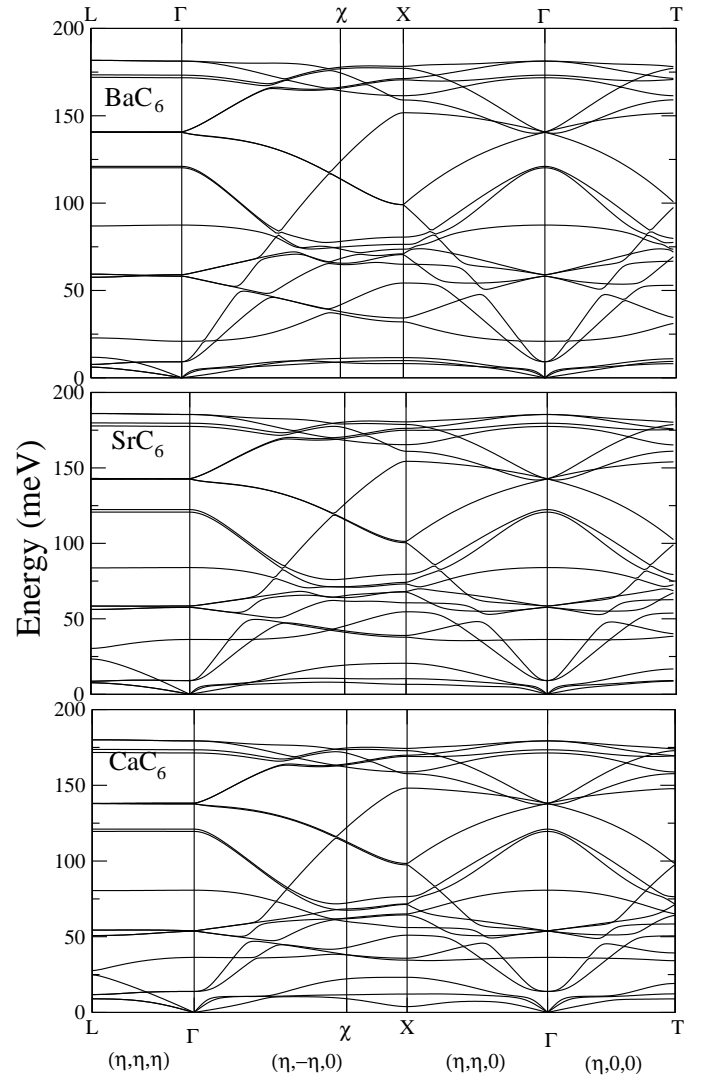


FIG. 4: Phonon dispersions of BaC_6 , SrC_6 and CaC_6 at 0 GPa.

derivative of the forces respect to the atomic displacements).

Using eq. 3 we decompose restricting the summation over i, j and that over i, j on two sets of atoms and Cartesian directions. The sets are C_{xy} , C_z , I_{xy} , and I_z , where $I = f\text{Ba, Sr, Ca}$. The resulting matrix for the different GICs and as a function of pressure are given in table III.

Except for of SrC_6 at 16.5 GPa, the off-diagonal matrix elements are negligible. In all the case the largest contributions to comes from C_z and I_{xy} phonon modes. The coupling to these modes are enhanced as Z and c are reduced. A similar enhancement of C_z and I_{xy} occurs under pressure. When the pressure is too high, as in SrC_6 at $P = 16.5$ GPa, the off-diagonal matrix elements increase and the attribution to C_z or to I_{xy} becomes ill-defined. Note also that the C_{xy} and the I_z modes are weakly affected by Z or c -axis reduction.

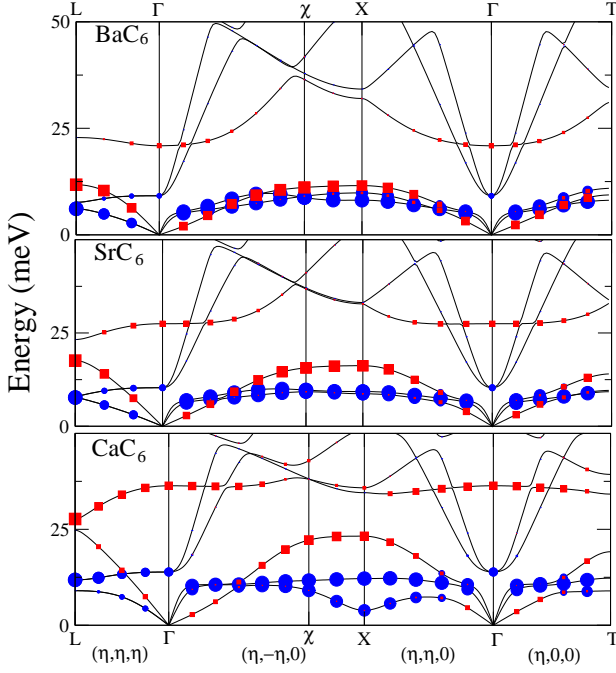


FIG. 5: (Color online) Low energy region of the phonon dispersions of BaC_6 , SrC_6 and CaC_6 at 0 GPa. The size of the blue dots (red squares) represents the amount of I_{xy} (I_z), where $I = \text{Ba;Sr;Ca}$ vibrations.

The critical superconducting temperature is estimated using the McMillan formula²⁵:

$$T_c = \frac{\hbar \omega}{1.2} e^{-\frac{1.04(1+\lambda)}{(1+0.62\lambda)}} \quad (4)$$

where λ is the screened Coulomb pseudopotential and

$$\hbar \omega = e^{\frac{2}{\pi} \int_0^{\infty} \frac{2F(\omega') \log(\omega')}{\omega'^2} d\omega'} \quad (5)$$

the phonon frequencies logarithmic average. Results for $\hbar \omega$ and for T_c are shown in table IV using $\lambda = 0.14$. For BaC_6 and SrC_6 , T_c increases as the interlayer spacing is decreased. For SrC_6 at 16.5 GPa the result of McMillan formula is not correct. Indeed close to the transition the increase in λ is only given by the softening of the Sr_{xy} vibration close to X. In McMillan formula the limit $\lambda \rightarrow 0$ implies $T_c \rightarrow 0$ although since $\lambda \rightarrow 1$ as $\lambda \rightarrow 0$. Unfortunately the use of McMillan formula in this limit is not correct since it deviates from the Migdal-Eliashberg results (ME), as known from the papers of McMillan²⁵ and of Allen and Dynes²⁶ (see e.g. 1 in²⁶). For this reason the calculation of T_c for SrC_6 at $P = 16.5$ GPa should be considered not reliable (and as a consequence it is not given in table IV).

VII. CaC_6 UNDER PRESSURE

The study of CaC_6 under pressure needs particular emphasis due to the interest motivated by the work of

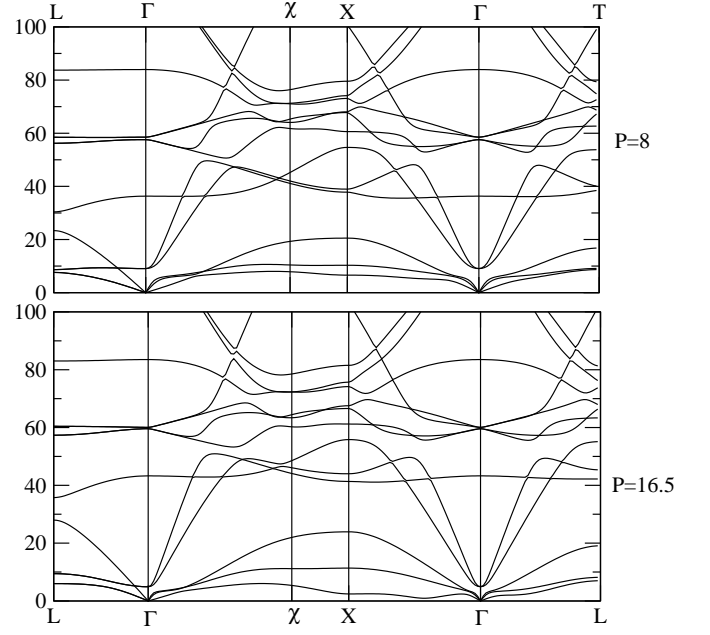


FIG. 6: Phonon dispersions of SrC_6 at 8 and 16.5 GPa.

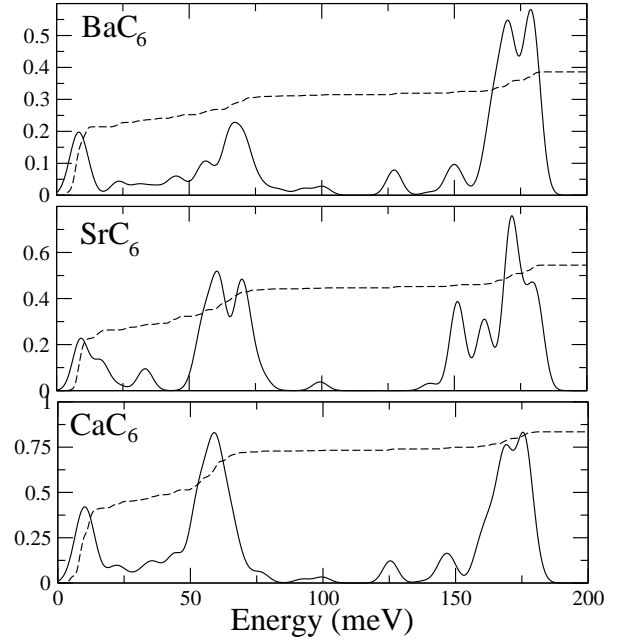


FIG. 7: (a) Zero-pressure Eliashberg function, $2F(\omega)$, (continuous line) and integrated coupling, $\lambda(\omega)$ (dashed) for BaC_6 , SrC_6 and CaC_6 .

Gauzzi et al.⁴ showing a considerable increase of T_c which reaches its maximum of 15.1 K at 7–8 GPa. The increase of T_c has been confirmed by other two successive works measuring T_c in a much smaller range of pressure^{17,18}. At 8 GPa the system seems to undergo a phase transition towards a different structure with a lower superconducting T_c .

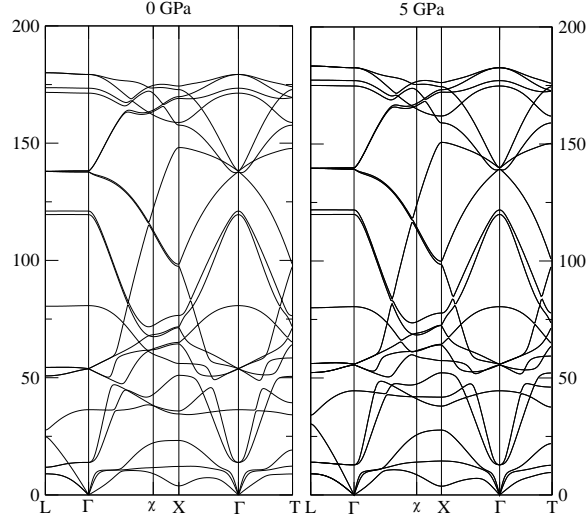


FIG. 8: Comparison between the phonon dispersion of CaC_6 at 0 GPa and at 5 GPa

To study the behavior of T_c under pressure we calculate the phonon dispersion and the electron-phonon coupling at 5 GPa, for which a $T_c = 14\text{ K}$ was detected in experiments. The comparison between the phonon dispersions at 0 GPa and 5 GPa is shown in Fig. 8. As can be seen, while the lowest Ca phonon mode is slightly softened (mostly at X), the others Ca and C_z phonon modes are hardened. However the overall change is fairly small and the Eliashberg functions $^2F(\omega)$ at 0 and 5 GPa have no sizable differences (see Fig. 9). At higher pressures the phonon frequencies become imaginary, similarly to what happens in SrC_6 at 16.5 GPa. In particular the largest softening occurs at X for the lowest Ca mode and it becomes negative in the range of 7-10 GPa. The lowest phonon frequency at X is extremely dependent on the Hermite-Gaussian smearing used in the calculation and as a consequence much larger k-point mesh must be used to correctly identify the phase transition (using a $10 \times 10 \times 10$ mesh and smearing 0.04 still gives results which are not converged). However it is clear that at a sufficient high pressure the system will become unstable and the lowest Ca phonon frequency at X will approach zero.

More insight on the superconducting properties can be gained by computing λ_{log} and ω_{log} at 0 and 5 GPa. In this range of pressures these parameters have very similar values and consequently the critical temperature changes only slightly (see table IV), from 11.03 K at 0 GPa to 11.40 K at 5 GPa.

The calculation for T_c under pressure are in stark disagreement with a recent theoretical calculation¹⁷ obtained using the same method (DFT) and the same code.

The disagreement with the calculation in ref.¹⁷ can be explained by the following. In ref.¹⁷ the electron-phonon coupling is calculated close to the structural transition (at 10 GPa) where the Ca phonon frequency strongly soft-

ens. Just before the structural transition, $\lambda_{\text{Ca}} \gg 0$ and consequently $\omega_{\text{Ca}} \gg 1$. In this limit (close to the transition), the behavior is highly non linear. On the contrary in ref.¹⁷ the behavior is assumed linear between 0 GPa and 10 GPa²⁷. Our calculation at 5.0 GPa giving essentially the same T_c as at 0 GPa shows that this is not the case.

We remark that in the calculation of the electron-phonon coupling at 0 and 5 GPa it is crucial to use at least a $4 \times 4 \times 4$ q-point mesh. If the smaller $2 \times 2 \times 2$ mesh is used, the electron-phonon coupling of the Ca modes is overestimated, since the point at X (which is included in the mesh and has a considerable electron-phonon coupling) has a too large weight. The consequent increase of T_c under pressure is much larger than in the $4 \times 4 \times 4$ mesh.

From the preceding discussion it follows that DFT calculations give a non linear behavior of T_c versus pressure, in stark disagreement with experiments. In particular the increase of T_c as a function of pressure is too weak when compared with experiments. In the next section we discuss what can be the origin of such disagreement.

VIII. CONCLUSIONS

In this work we theoretically investigated the occurrence of superconductivity in graphite intercalated with Alkaline earths (in particular BaC_6 , SrC_6 , MgC_6). Most of these systems have been already synthesized (BaC_6 , SrC_6 and CaC_6), while MgC_6 has been proposed¹⁰ as a good candidate for superconductivity due to its light mass and small force constants, possibly leading to large electron-phonon coupling.

We predict the critical temperatures of BaC_6 and SrC_6 to be 0.23 K and 3.02 K respectively. Moreover we also

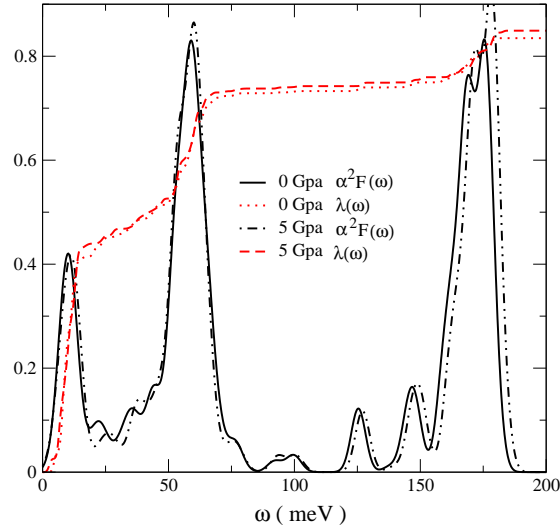


FIG. 9: (Color online) Comparison between $\alpha^2F(\omega)$ and $\lambda(\omega)$ at 0 GPa and 5 GPa for CaC_6 .

predict a substantial increase in the critical temperature under pressure for these two systems, namely at 8 GPa the critical estimated temperatures for BaC_6 and SrC_6 are 0.81 K and 5.16 K respectively. We hope that these predictions can stimulate additional experimental work so that the nature of the pairing in GICs can be further elucidated. Moreover it would be important to judge the reliability of DFT in calculating the superconducting properties of different GICs. Indeed, while superconducting gap and specific heat measurements are in very good agreement with DFT calculations the only available measure of the Ca isotope effect¹⁶ in CaC_6 is in stark disagreement with DFT predictions¹¹. The claim that the isotope effect coefficient of Ca is 0.5, if verified by the corresponding measurement of the C isotope effect, would open new perspectives.

We have also shown that MgC_6 is energetically unstable against phase separation in Mg and graphite. Moreover, even assuming that it can be synthesized using pressure methods, the minimized structure at zero pressure obtained using DFT has imaginary phonon frequencies at the point X. Nonetheless it is interesting to note that the softening at the point X occurs when the interlayer spacing is reduced in CaC_6 and is connected to a large electron-phonon coupling in this point. This information suggests that the T_c of CaC_6 can probably be raised synthesizing $\text{Mg}_x\text{Ca}_{1-x}\text{C}_y$ alloys.

Concerning CaC_6 , a puzzling problem is the dependence of the critical superconducting temperature upon pressure. Experimentally T_c increases as a function of pressure, but as we have shown in this work, T_c increases much faster than what DFT calculations predict. Further work is necessary to explain the origin of this

disagreement, mainly on the experimental side. Indeed diffraction data as a function of pressure are absolutely necessary. If there is a phase transformation upon pressure, the structure minimized with DFT at finite pressure would not be correct. The fact that the T_c versus pressure curves are very smooth seems to exclude an abrupt transition. A possibility is that a staging transition occurs in CaC_6 under pressure. This transition could be continuous, meaning that the staging occurs progressively in the sample. It is indeed well known that GICs are extremely sensitive to these kind of transitions occurring isothermally under very modest pressures. For example KC_{24} , which is a stage 2 GIC, starts a staging transition at 2.5 Kbar versus a stage 3 structure. The transition is continuous and completely achieved at 6.5 Kbar²⁸. Similar transitions have been reported in ref.²⁹ for MC_8 and MC_{12n} ($n=2,3,4$) with $M=\text{Rb}, \text{Cs}$. If such a transition occurs in CaC_6 then it would not necessarily show up in the T_c versus pressures curves, but it would explain the disagreement between experiment and theory. Of course other more complicated explanations are possible, including unconventional superconductivity. In all the case, the origin of superconductivity in intercalated GICs is not yet completely understood.

IX. ACKNOWLEDGEMENTS

We acknowledge fruitful discussion with A. G. Auzzi, G. Loupias, M. d'Astuto, N. Emery, C. Herold and L. Boeri. Calculations were performed at the IDRIS supercomputing center (project 061202).

¹ M. S. Dresselhaus and G. Dresselhaus, *Adv. in Phys.* **51**, 1, 2002

² T. E. Weller, M. Ellerby, S. S. Saxena, R. P. Smith and N. T.

C ₆ Ba P=0				
	C _{xy}	C _z	Ba _{xy}	Ba _z
C _{xy}	0.10	0.00	-0.01	0.00
C _z	0.00	0.10	0.01	-0.01
Ba _{xy}	-0.01	0.01	0.12	-0.00
Ba _z	0.00	-0.01	0.00	0.07
C ₆ Ba P=8				
	C _{xy}	C _z	Ba _{xy}	Ba _z
C _{xy}	0.10	0.01	-0.00	0.00
C _z	0.01	0.11	0.02	-0.01
Ba _{xy}	-0.00	0.02	0.16	-0.00
Ba _z	0.00	-0.01	-0.00	0.05
C ₆ Sr P=0				
	C _{xy}	C _z	Sr _{xy}	Sr _z
C _{xy}	0.12	0.00	-0.00	0.00
C _z	0.00	0.20	0.02	-0.00
Sr _{xy}	-0.00	0.02	0.16	-0.00
Sr _z	0.00	-0.00	-0.00	0.05
C ₆ Sr P=8				
	C _{xy}	C _z	Sr _{xy}	Sr _z
C _{xy}	0.12	0.01	-0.00	0.00
C _z	0.01	0.24	0.03	-0.01
Sr _{xy}	-0.00	0.03	0.19	-0.00
Sr _z	0.00	-0.01	-0.00	0.04
C ₆ Sr P=16				
	C _{xy}	C _z	Sr _{xy}	Sr _z
C _{xy}	0.13	0.03	-0.01	0.00
C _z	0.03	0.65	0.21	-0.01
Sr _{xy}	-0.01	0.21	0.71	-0.04
Sr _z	0.00	-0.01	-0.04	0.12
C ₆ Ca P=0				
	C _{xy}	C _z	Ca _{xy}	Ca _z
C _{xy}	0.12	0.00	-0.00	0.00
C _z	0.00	0.33	0.04	-0.01
Ca _{xy}	-0.00	0.04	0.27	-0.00
Ca _z	0.00	-0.01	-0.00	0.06
C ₆ Ca P=5				
	C _{xy}	C _z	Ca _{xy}	Ca _z
C _{xy}	.13	.01	-.00	.00
C _z	.01	.35	.03	-.01
Ca _{xy}	-.00	.03	.26	-.01
Ca _z	.00	-.01	-.01	.05

TABLE III: Decomposition of the electron-phonon coupling parameter into different vibrational components for several GICs

C ₆ Ba			
P (GPa)	$\ln T_c$ (m eV)	T_c (K)	(= 0.14) K
0	0.38	22.44	.23
8	0.45	20.63	.81
C ₆ Sr			
P (GPa)	$\ln T_c$ (m eV)	T_c (K)	(= 0.14) K
0	0.54	28.38	3.03
8	0.65	23.40	5.17
16.5	1.97	3.67	nonsense
C ₆ Ca			
P (GPa)	$\ln T_c$ (m eV)	T_c (K)	(= 0.14) K
0	0.83	24.70	11.03
5	0.845	24.6	11.40

TABLE IV: Superconducting parameters of several GICs under pressure

- Skipper, Nature Phys. 1, 39 (2005) and cond-m at/0503570
- ³ N. Emery, C. Herold, M. d'Astuto, V. Garcia, Ch. Bellin, J. F. M. arêche, P. Lagrange and G. Loupîas, Phys. Rev. Lett. 95, 087003 (2005)
- ⁴ A. Gauzzi, S. Takashima, N. Takeshita, C. Terakura, H. Takagi, N. Emery, C. Herold, P. Lagrange, G. Loupîas, cond-m at/0603443
- ⁵ O. Gunnarsson, Rev. Mod. Phys. 69, 575-606 (1997)
- ⁶ E. A. Ekimov et al. Nature (London), 428, 542 (2004)
- ⁷ Z. K. Tang, L. Zhang, N. Wang, X. X. Zhang, G. H. Wen, G. D. Li, J. N. Wang, C. T. Chan, P. Sheng, Science 292, 2462 (2001)
- ⁸ G. Csanyi, P. B. Littlewood, A. H. Nevidomskyy, C. J. Pickard and B. D. Simons, Nature Physics 1, 42 (2005) and cond-m at/0503569

- ⁹ D. Allender, J. Bray and J. Bardeen, PRB 7, 1020 (1973)
- ¹⁰ I. I. Mazin Phys. Rev. Lett. 95, 227001 (2005)
- ¹¹ M. Calandra and F. Mauri, Phys. Rev. Lett. 95, 237002 (2005)
- ¹² G. Lamura, M. Aurino, G. Cifariello, E. Di Gennaro, A. Andreone, N. Emery, C. Herold, J. F. M. arêche and P. Lagrange, cond-m at/0601339
- ¹³ N. Bergeal, V. Dubost, Y. Noat, W. Sacks, D. Roditchev, N. Emery, C. Herold, J. F. M. arêche P. Lagrange and G. Loupîas, cond-m at/0604208
- ¹⁴ J. S. Kim, R. K. Krammer, L. Boeri, F. S. Razavi, cond-m at/0603539
- ¹⁵ M. Sutherland, N. Doiron-Leyraud, L. Taillefer, T. Weller, M. Ellerby, S. S. Saxena, cond-m at/0603664
- ¹⁶ D. G. Hinks, D. Rosenmann, H. Claus, M. S. Bailey, and J. D. Jorgensen, cond-m at/0604642
- ¹⁷ J. S. Kim, L. Boeri, R. K. Krammer, F. S. Razavi, cond-m at/0603530
- ¹⁸ R. P. Smith, A. Kuznetsova, Y. T. C. Ko, S. S. Saxena, A. Akrap, L. Forro, M. Laad, T. E. Weller, M. Ellerby, N. T. Skipper, cond-m at/0604204
- ¹⁹ <http://www.pwscf.org>, S. Baroni, et al., Rev. Mod. Phys. 73, 515-562 (2001)
- ²⁰ J. P. Perdew, K. Burke, M. Ernzerhof, Phys. Rev. Lett. 77, 3865 (1996)
- ²¹ D. Vanderbilt, PRB 41, 7892 (1990)
- ²² N. Troullier and J. L. Martins, Phys. Rev. B 43, 1993 (1991).
- ²³ D. Gurard, M. Chaabouni, P. Lagrange, M. Elmakrini et A. Herold, Carbon 18 (1980) 257-264
- ²⁴ The results for SrC₆ at 16.5 GPa should be considered only qualitative since much larger q- and k-points mesh should be used. Moreover very close to the structural instability anharmonic effects might become relevant.
- ²⁵ McMillan, Phys. Rev. 167, 331 (1968).
- ²⁶ P. B. Allen and R. C. Dynes, Phys. Rev. B 12, 905-922 (1975)
- ²⁷ Even assuming a linear behavior, the theoretical T_c versus pressure slope is substantially smaller than the experimental one.
- ²⁸ R. Clarke, N. Wada and S. A. Solin, Phys. Rev. Lett. 44, 1616 (1980)
- ²⁹ N. Wada, Phys. Rev. B 24 1065 (1981)